

New Insights into the Vacuum UV Photodissociation of Peptides

Ramakrishnan Parthasarathi, Yi He, James P. Reilly, and Krishnan Raghavachari*

Department of Chemistry, Indiana University, Bloomington, Indiana 47405

Received September 23, 2009; E-mail: kraghava@indiana.edu

Abstract: Vacuum ultraviolet laser photodissociation (UVPD) of peptide ions leads to unusual dissociation channels involving backbone C–C bond breaking. However, the molecular basis for the observed behavior is not clearly understood. We now report theoretical investigations using ab initio/density functional theory (DFT) techniques on neutral and protonated dipeptides undergoing vacuum ultraviolet (VUV) induced fragmentation via a Rydberg excitation (and/or electron detachment) and subsequent C–C bond cleavage. New experimental results on VUV photodissociation of dipeptides (protonated Ala₂Arg and Arg₂Ala) provide strong support for our proposed model. Our mechanism also provides a natural explanation for the presence of immonium ions that are sometimes observed in such experiments.

Introduction

Following immense progress made in the last century, it may reasonably be claimed that today the frontier of research in the area of protein science lies at the boundary between chemistry, biology, medicine, and materials science. One active area of research in mass spectrometry (MS) and proteomics involves studies of the dissociation of peptide ions.^{1–15} There are a variety of peptide ion fragmentation methodologies available for interrogating peptides including blackbody radiation,¹ IR multiphoton excitation,² UV laser excitation,^{3,4} and collisions with gas-phase molecules or surfaces.⁵ Most of these are low-energy activation approaches in which excitation is introduced incrementally on a time scale that is long compared to that of intramolecular relaxation. Thus, ions are effectively thermally excited. In this case, gas-phase fragmentation of protonated

peptides is typically dominated by cleavages of peptide (amide) bonds resulting in the formation of characteristic *b* and *y* ions (Scheme 1 in the Supporting Information).⁶ Loss of small molecules such as NH₃ and H₂O from precursor and fragment ions is also commonly observed in tandem mass spectra. In contrast, high-energy (beam-type) collisional activation of peptide ions can lead to other types of backbone cleavages and the production of internal fragments and immonium ions from simultaneous or consecutive rupture of two peptide bonds. Mechanisms for the formation of these fragments in high-energy

- (1) Price, W. D.; Schnier, P. D.; Williams, E. R. *Anal. Chem.* **1996**, *68*, 859–866.
- (2) Zimmerman, J. A.; Watson, C. H.; Eyler, J. R. *Anal. Chem.* **1991**, *63*, 361–365.
- (3) Bowers, W. D.; Delbert, S. S.; Hunter, R. L.; McIver, R. T. *J. Am. Chem. Soc.* **1984**, *106*, 7288–7289. Martin, S. A.; Hill, J. A.; Kittrell, C.; Biemann, K. *J. Am. Soc. Mass Spectrom.* **1990**, *1*, 107–109. Williams, E. R.; Furlong, J. J.; McLafferty, F. W. *J. Am. Soc. Mass Spectrom.* **1990**, *1*, 288–294. Gorman, G. S.; Amster, I. J. *Org. Mass Spectrom.* **1993**, *9*, 437–444. Gimonkinkel, M. E.; Kinsel, G. R.; Edmondson, R. D.; Russell, D. H. *J. Am. Soc. Mass Spectrom.* **1995**, *6*, 578–587. Nikogosyan, D. H.; Gorner, H. *Biol. Chem.* **1997**, *378*, 1349–1351. Barbacci, D. C.; Russell, D. H. *J. Am. Soc. Mass Spectrom.* **1999**, *10*, 1038–1040. Oh, J. Y.; Moon, J. H.; Kim, M. S. *J. Am. Soc. Mass Spectrom.* **2004**, *15*, 1248–1259.
- (4) Thompson, M. S.; Cui, W. D.; Reilly, J. P. *Angew. Chem., Int. Ed.* **2004**, *43*, 4791–4794. Cui, W. D.; Thompson, M. S.; Reilly, J. P. *J. Am. Soc. Mass Spectrom.* **2005**, *16*, 1384–1398. Thompson, M. S.; Cui, W. D.; Reilly, J. P. *J. Am. Soc. Mass Spectrom.* **2007**, *18*, 1439–1452. Reilly, J. P. *Mass Spectrom. Rev.* **2009**, *28*, 425–447.
- (5) Hunt, D. F.; Bone, W. M.; Shabanowitz, J.; Rhodes, J.; Ballard, J. M. *Anal. Chem.* **1981**, *53*, 1704–1706. Williams, E. R.; Henry, K. D.; McLafferty, F. W.; Shabanowitz, J.; Hunt, D. F. *J. Am. Soc. Mass Spectrom.* **1990**, *1*, 413–416.
- (6) Biemann, K. *Mass Spectrometry, Organic Chemical Applications*; McGraw-Hill: New York, 1962; Chapter 7. Biemann, K.; Martin, S. A. *Mass Spectrom. Rev.* **1987**, *6*, 1–75. Johnson, R. S.; Martin, S. A.; Biemann, K. *Int. J. Mass Spectrom. Ion Processes* **1988**, *86*, 137–154. Biemann, K. *Biomed. Environ. Mass Spectrom.* **1988**, *16*, 99. Biemann, K. *Methods Enzymol.* **1990**, *193*, 351–360, 455–479.
- (7) Csonka, I. P.; Paizs, B.; Lendvay, G.; Suhai, S. *Rapid Commun. Mass Spectrom.* **2000**, *14*, 417–431. Paizs, B.; Suhai, S. *Rapid Commun. Mass Spectrom.* **2001**, *15*, 2307–2323. Csonka, I. P.; Paizs, B.; Lendvay, G.; Suhai, S. *Rapid Commun. Mass Spectrom.* **2001**, *15*, 1457–1472. Paizs, B.; Csonka, I. P.; Lendvay, G.; Suhai, S. *Rapid Commun. Mass Spectrom.* **2001**, *15*, 637–650. Paizs, B.; Suhai, S. *Rapid Commun. Mass Spectrom.* **2002**, *16*, 375–389. Paizs, B.; Schnolzer, M.; Warnken, U.; Suhai, S.; Harrison, A. G. *Phys. Chem. Chem. Phys.* **2004**, *6*, 2691–2699. Paizs, B.; Suhai, S. *J. Am. Soc. Mass Spectrom.* **2004**, *15*, 103–113. Paizs, B.; Suhai, S. *Mass Spectrom. Rev.* **2005**, *24*, 508–548.
- (8) McCormack, A. L.; Somogyi, A.; Dongre, A. R.; Wysocki, V. H. *Anal. Chem.* **1993**, *65*, 2859–2872. Jones, J. L.; Dongre, A. R.; Somogyi, A.; Wysocki, V. H. *J. Am. Chem. Soc.* **1994**, *116*, 8368–8369. Dongre, A. R.; Jones, J. L.; Somogyi, A.; Wysocki, V. H. *J. Am. Chem. Soc.* **1996**, *118*, 8365–8374. Wysocki, V. H.; Tsapralis, G.; Smith, L. L.; Breci, L. A. *J. Mass Spectrom.* **2000**, *35*, 1399–1406. Wysocki, V. H.; Resing, K. A.; Zhang, Q. F.; Cheng, G. L. *Methods* **2005**, *35*, 211–222. Komaromi, I.; Somogyi, A.; Wysocki, V. H. *Int. J. Mass Spectrom.* **2005**, *241*, 315–323.
- (9) Alexander, A. J.; Thibault, P.; Boyd, R. K. *Rapid Commun. Mass Spectrom.* **1989**, *3*, 30–35. Ballard, K. D.; Gaskell, S. J. *Int. J. Mass Spectrom. Ion Processes* **1991**, *111*, 173–189. Burrell, O.; Yang, C. Y.; Gaskell, S. J. *J. Am. Soc. Mass Spectrom.* **1992**, *3*, 337–344. Bolgar, M. S.; Gaskell, S. J. *Biochem. Soc. Trans.* **1995**, *23*, 907–910. Cox, K. A.; Gaskell, S. J.; Morris, M.; Whiting, A. *J. Am. Soc. Mass Spectrom.* **1996**, *7*, 522–531.
- (10) Tsang, C. W.; Harrison, A. G. *J. Am. Chem. Soc.* **1976**, *98*, 1301–1308. Forbes, M. W.; Jockusch, R. A.; Young, A. B.; Harrison, A. G. *J. Am. Soc. Mass Spectrom.* **2007**, *18*, 1959–1966. Bleiholder, C.; Osburn, S.; Williams, T. D.; Suhai, S.; Van Stipdonk, M.; Harrison, A. G.; Paizs, B. *J. Am. Chem. Soc.* **2008**, *130*, 17774–17789.
- (11) Barlow, C. K.; O'Hair, R. A. J. *J. Mass Spectrom.* **2008**, *43*, 1301–1319. O'Hair, R. A. J.; Broughton, P. S.; Styles, M. L.; Frink, B. T.; Hadad, C. M. *J. Am. Soc. Mass Spectrom.* **2000**, *11*, 687–696. Wee, S.; O'Hair, R. A. J.; McFadyen, W. D. *Int. J. Mass Spectrom.* **2004**, *234*, 101–122.

collisional activation experiments have been previously described by the Biemann group.⁶ Our current understanding of gas-phase ion chemistry associated with fragmentation of peptide ions has been summarized in a number of articles and recent reviews.^{4–15}

Vacuum ultraviolet laser photodissociation (VUVPD) is an elegant, high-energy method for inducing fragmentation in peptides. Following electronic excitation, direct dissociation in the excited state competes with radiative relaxation and internal conversion to the electronic ground state. Direct fragmentation is possible because the photon energies are higher than bond strengths in peptides.¹⁶ Experimental and theoretical work have shown that small peptides have strong absorption bands in the vacuum ultraviolet associated with backbone chromophores. Reilly and co-workers have studied the photodissociation of protonated peptides using 157 nm (7.9 eV) vacuum UV (VUV) light.⁴ This high-energy activation results in formation of x , v , and w fragments when a basic arginine (Arg) residue is located at the C-terminus of the peptide, and a and d ions for peptides with N-terminal arginine. They rationalized these observations using a mechanism that involves homolytic C–C radical cleavage via a Norrish type I reaction followed by radical elimination processes from the primary radical cations.⁴ According to this mechanism, a - and x -type ions are formed by removal of a hydrogen atom from the corresponding $a + 1$ and $x + 1$ radical precursors. In earlier studies using high-energy collision-induced dissociation of peptide ions, Biemann and co-workers have proposed mechanisms for fragmentation processes leading to a variety of daughter ions.⁶

Several groups have performed similar experiments with 193 nm light, but the resulting fragmentation patterns exhibit significant variations.^{3,17} Despite the importance of peptide photodissociation in protein analysis, VUV-induced fragmentation of protonated peptides is implicitly understood only at an

empirical level. This is in contrast with other dissociation methods for peptides; for example, the “mobile proton” model provides a good understanding of the low-energy fragmentation of protonated peptides.^{7–9} High-energy fragmentation pathways^{10,11} such as charge-remote peptide fragmentation mechanisms¹² have also been explored in some cases. Similarly, mechanisms to understand electron capture dissociation involving protonated and deprotonated peptides have also been proposed.^{13–15} In this article, theoretical investigations will be focused on understanding VUV laser-induced dissociation of peptides.

Computational Details

Dipeptide model systems are ideal candidates for the theoretical study of laser-induced chemistry; they are simple enough to treat using a reasonable quantum chemical approach, yet complex enough to display experimentally observed fragmentation behavior. The geometry optimizations of dipeptides (as neutral or protonated singlet forms) and their ionized doublet states reported in this communication were performed using density functional theory (DFT) with the B3LYP hybrid exchange-correlation functional and the 6-311++G(d,p) basis set.¹⁸ Low-energy conformations were studied in all cases and were confirmed to be minima by means of frequency calculations. Rigid potential energy surface scan calculations (along C–C, C–N, and N–C bond coordinates) have been carried out for both forms. In addition, MP2/6-311++G(d,p) optimizations were done to validate the general conclusions from the DFT calculations. Calculations were carried out of the selected dipeptides to locate many local minima because of numerous conformational degrees of freedom. We have reported the best minima achieved by our calculations.

Experimental Section

The dipeptides Ala_Arg and Arg_Ala were diluted to 20 pmol/ μ L with H₂O, and then, 0.5 μ L of this solution was spotted on a matrix-assisted laser desorption/ionization (MALDI) target plate. When the spots were dry, 0.5 μ L of matrix solution (2.5 mg/mL CHCA in 50% ACN/50% H₂O/0.1% trifluoroacetic acid) was applied on top of it.

MALDI mass spectra were recorded on an ABI 4700 TOF-TOF mass spectrometer (Foster City, CA). All measurements were performed in positive reflectron mode. For the photodissociation experiments, an F₂ laser (Coherent Lambda Physik, Germany) is connected to the ABI 4700 TOF-TOF mass spectrometer as recently described.¹⁹ Its timing is automatically controlled by a programmable delay generator.

Results and Discussion

The direct study of high-lying electronic excited states is a challenging problem. This is particularly difficult due to the presence of a large number of excited states at 8 eV and the potential for substantial Rydberg-valence mixing at these high energies. In particular, VUV radiation is known to excite high-lying Rydberg-type states for many systems (while near UV light does not).²⁰ It is generally recognized that the principal characteristics of such excited states are similar to those of the corresponding cations. Since the excited electron in Rydberg

- (12) Jensen, N. J.; Tomer, K. B.; Gross, M. L. *J. Am. Chem. Soc.* **1985**, *107*, 1863–1868. Hayes, R. N.; Gross, M. L. *Methods Enzymol.* **1990**, *193*, 237–263. Gross, M. L. *Int. J. Mass Spectrom. Ion Processes* **1992**, *118/119*, 137–165. Cheng, C. F.; Pittenauer, E.; Gross, M. L. *J. Am. Soc. Mass Spectrom.* **1998**, *9*, 840–844. Cheng, C. F.; Gross, M. L. *Mass Spectrom. Rev.* **2000**, *19*, 398–420. Gross, M. L. *Int. J. Mass Spectrom.* **2000**, *200*, 611–624.
- (13) Zubarev, R. A.; Haselmann, K. F.; Budnik, B.; Kjeldsen, F.; Jensen, F. *Eur. J. Mass Spectrom.* **2002**, *8*, 337–349. Kjeldsen, F.; Silivra, O. A.; Ivonin, I. A.; Haselmann, K. F.; Gorshkov, M.; Zubarev, R. A. *Chem.—Eur. J.* **2005**, *11*, 1803–1812. Kjeldsen, F.; Silivra, O. A.; Zubarev, R. A. *Chem.—Eur. J.* **2006**, *12*, 7920–7928. Zubarev, R. A.; Zubarev, A. R.; Savitski, M. M. *J. Am. Soc. Mass Spectrom.* **2008**, *19*, 753–761.
- (14) Turecek, F. *J. Am. Chem. Soc.* **2003**, *125*, 5954–5963. Syrtstad, E. A.; Turecek, F. *J. Am. Soc. Mass Spectrom.* **2005**, *16*, 208–224. Chen, X. H.; Turecek, F. *J. Am. Chem. Soc.* **2006**, *128*, 12520–12530. Chamot-Rooke, J.; Malosse, C.; Frison, G.; Turecek, F. *J. Am. Soc. Mass Spectrom.* **2007**, *18*, 2146–2161. Chung, T. W.; Turecek, F. *Eur. J. Mass Spectrom.* **2008**, *14*, 367–378. Turecek, F.; Chen, X. H.; Hao, C. T. *J. Am. Chem. Soc.* **2008**, *130*, 8818–8833.
- (15) Anusiewicz, I.; Jasionowski, M.; Skurski, P.; Simons, J. *J. Phys. Chem. A* **2005**, *109*, 11332–11337. Anusiewicz, I.; Sobczyk, M.; Berdys-Kochanska, J.; Skurski, P.; Simons, J. *J. Phys. Chem. A* **2005**, *109*, 484–492. Anusiewicz, W.; Berdys-Kochanska, J.; Simons, J. *J. Phys. Chem. A* **2005**, *109*, 5801–5813. Sobczyk, M.; Anusiewicz, W.; Berdys-Kochanska, J.; Sawicka, A.; Skurski, P.; Simons, J. *J. Phys. Chem. A* **2005**, *109*, 250–258. Anusiewicz, I.; Berdys-Kochanska, J.; Skurski, P.; Simons, J. *J. Phys. Chem. A* **2006**, *110*, 1261–1266. Sobczyk, M.; Simons, J. *J. Phys. Chem. B* **2006**, *110*, 7519–7527.
- (16) Preiss, J. W.; Setlow, R. *J. Chem. Phys.* **1956**, *25*, 138–141.
- (17) Moon, J. H.; Yoon, S. H.; Kim, M. S. *Rapid Commun. Mass Spectrom.* **2005**, *19*, 3248–3252. Choi, K. M.; Yoon, S. H.; Sun, M. L.; Oh, J. Y.; Moon, J. H.; Kim, M. S. *J. Am. Soc. Mass Spectrom.* **2006**, *17*, 1643–1653. Moon, J. H.; Shin, Y. S.; Cha, H. J.; Kim, M. S. *Rapid Commun. Mass Spectrom.* **2007**, *21*, 359–368.

- (18) Frisch, M. J. T.; et al. Gaussian DV, Revision G.01; Gaussian Inc: Wallingford, CT, 2007.
- (19) Zhang, L.; Reilly, J. P. *Anal. Chem.* **2009**, *81*, 7829–7838.
- (20) Zhu, L.; Johnson, P. *J. Chem. Phys.* **1991**, *94*, 5769–5771. Merkt, F.; Zare, R. N. *J. Chem. Phys.* **1994**, *101*, 3495–3505. Held, A.; Schlag, E. W. *Acc. Chem. Res.* **1998**, *31*, 467–473. Sándorfy, C. *The Role of Rydberg States in Spectroscopy and Photochemistry. Low and High Rydberg States*; Kluwer Academic Publishers: Dordrecht, The Netherlands, 1999; Vol. 20. Softley, T. P. *Int. Rev. Phys. Chem.* **2004**, *23*, 1–78. Fedorov, I.; Koziol, L.; Li, G.; Reisler, H.; Krylov, A. I. *J. Phys. Chem. A* **2007**, *111*, 13347–13357.

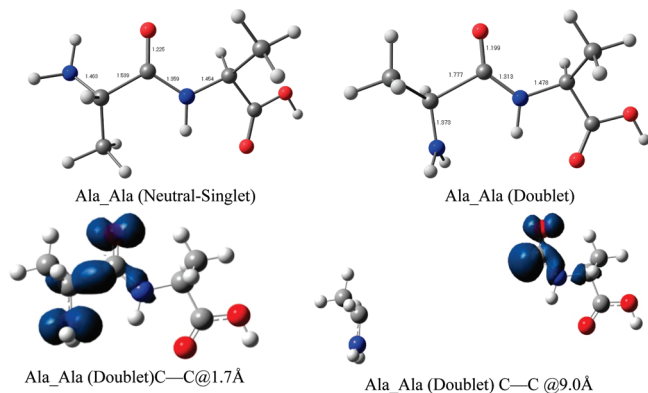


Figure 1. B3LYP/6-311++G(d,p) optimized geometries for the neutral and ionized forms of the Ala_Ala dipeptide. Calculated bond distances (Å) are shown. The unpaired electron (spin) densities of the cation at equilibrium (left) and a stretched bond length (right) are also shown.

states occupies a diffuse orbital, the structure and properties of molecules in such states should be similar to those in the corresponding cations. In fact, high-resolution spectroscopic methods such as zero kinetic energy photoelectron spectroscopy (ZEKE) and mass analyzed threshold ionization spectroscopy (MATI) are predicated on the proposition that high Rydberg states have spectra similar to those of the corresponding ions.²⁰ Computationally, while convergence to specific high-lying Rydberg states is often difficult to achieve, it is much easier to study the properties of the cations. We find that many of the experimental observations on 157 nm laser-induced fragmentation⁴ can be explained by a careful analysis of such cations and their associated fragmentation behavior. In particular, their unusual fragmentation involving C–C bond breaking as well as immonium ion formation even with small peptides are explained naturally by our analysis.

The essential points of our analysis can be illustrated by the behavior of the simple alanine dipeptide (Ala_Ala). The geometries of the neutral dipeptide and the corresponding cation are shown in Figure 1. The corresponding spin density distribution is also shown in Figure 1. Three types of backbone bonds are present in every peptide: C–C, C–N, and N–C. While the C–C bond is the weakest of the three (for neutral peptides), it is the peptide bond (C–N) that breaks under low-energy collision activated conditions for protonated peptides. This is elegantly explained by the “mobile proton” model that states that, upon ion activation, the proton migrates to the available protonation sites prior to fragmentation and will facilitate charge-directed cleavages.^{6–9} In particular, protonation of the amide nitrogen makes the peptide bond weaker than the C–C bond, leading to C–N bond breaking under low-energy (“thermal”) conditions. The results are however very different following VUV excitation of a Rydberg state (that, once again, we model as an ion). It is immediately evident that the C–C bond is weakened substantially in the cation, clearly suggesting that the electron being excited in the Rydberg state comes from the corresponding bonding orbital. The unpaired electron spin density distribution in the cation is consistent with this analysis and exhibits significant character in the vicinity of the C–C bond (Figure 1). By using a large 6-311++G(d,p) basis set, the bond is stretched by nearly 0.23 Å. The C–C bond strength decreases from 71 kcal/mol in the neutral to 17 kcal/mol in the cation. The weakening of that bond as seen in the energy profile (Figure 2) clearly facilitates C–C peptide backbone cleavage.

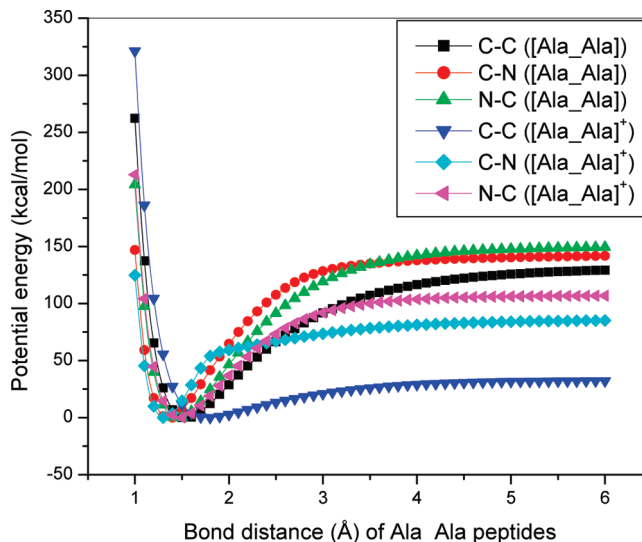


Figure 2. Potential energy surfaces of bond dissociation in Ala_Ala peptides. The scans were carried out by stretching the bond distances while keeping the remaining parameters constant.

Experiments on 157 nm UV-induced dissociation of peptide ions are typically carried out with arginine near the C- or N-termini.⁴ C–C bond breaking is the dominant mode observed experimentally with the charge usually sequestered on the arginine. While most of the experimentally investigated peptides are much larger, we have performed calculations on two dipeptides containing protonated arginine, Ala_Arg(H)⁺ and (H)⁺Arg_Ala. Geometrical parameters of the Ala_Arg(H)⁺ and (H)⁺Arg_Ala peptide ions in their ground (i.e., protonated) and ionized (i.e., doubly charged) states are shown in Figure 3. Again, the ionized state displays a dramatic elongation of the C–C bond, exactly analogous to the behavior seen earlier for the neutral dipeptide Ala_Ala. Calculations were carried out on the selected dipeptide model systems in both the states to locate many local minima. The most stable peptide ion conformers in the ground state for Ala_Arg are stabilized by intramolecular hydrogen bonding to the amide carbonyl (folded conformation) or carboxyl terminal (unfolded conformation). The unfolded conformation is 3.4 kcal/mol stable than the folded conformer. For Arg_Ala peptide ions, the most stable conformation is stabilized by intramolecular hydrogen bonding to the amide carbonyl. While there are many conformations, it is worth emphasizing here that C–C bond elongation and weakening on electron detachment is completely independent of the conformation used. Investigation of many other dipeptides shows this to be a very general and important finding: the ionized state (analogous to the high Rydberg states) is notably more elongated along the C–C bond than the corresponding ground state.

In order to carry out a direct comparison with our theoretical results, the two protonated dipeptides, Ala_Arg(H)⁺ and (H)⁺Arg_Ala, were investigated experimentally, and their 157 nm photodissociation spectra are displayed in Figure 4. These two spectra are quite clean with only one major fragment ion in each. In the case of Ala_Arg, the proton is sequestered on the C-terminal arginine. As shown in the spectrum (Figure 4A), an x_1 ion is generated when the C–C bond is cleaved. In the case of Arg_Ala (Figure 4B), the proton is on the N-terminal arginine, and a_1 is the major fragment ion produced by the photodissociation process. Similar to previously reported results on larger peptide photodissociation,⁴ the spectrum is dominated by an x -type ion in the case of the Ala_Arg peptide cation and

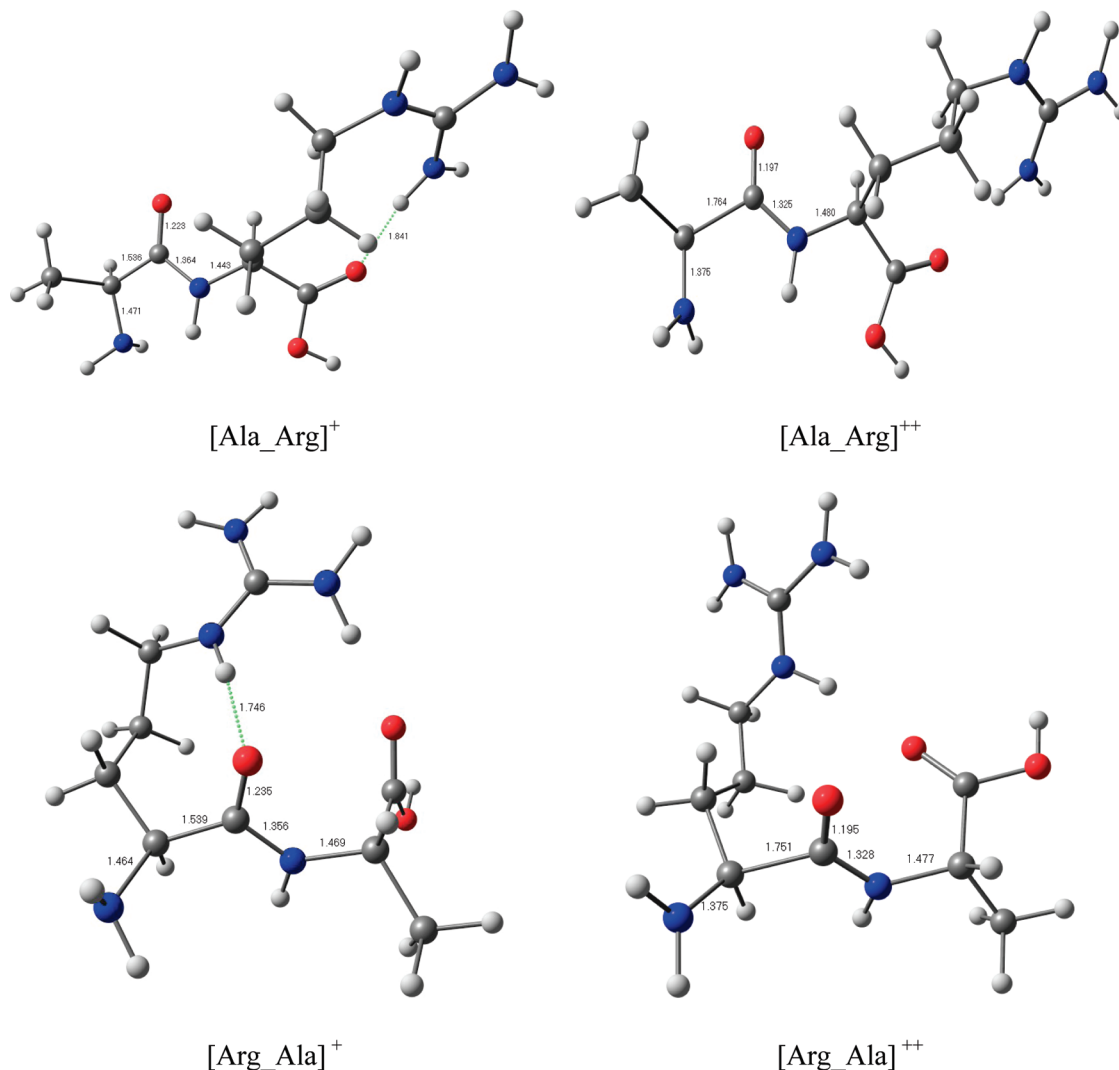


Figure 3. B3LYP/6-311++G(d,p) optimized geometries of peptide ions with terminal arginine.

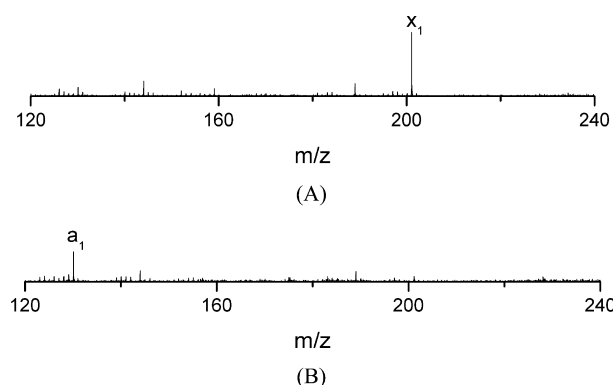


Figure 4. 157 nm photodissociation spectra of dipeptides (A) $[\text{Ala_Arg}]^+$ and (B) $[\text{Arg_Ala}]^+$.

an a -type of ion for the Arg_Ala peptide ion. The x - and a -type ions correspond to cleavage of backbone $\text{C}_\alpha\text{--C}(\text{O})$ bonds with the charge retained on the C- and N-terminal arginines, respectively. In this context, we point out that the traditional peptide bond breaking mechanism can also yield the a_1 ion via CO loss from the initially formed b_1 ion. However, the dominant presence of the x_1 ion cannot be explained by peptide bond breaking and offers direct support for the C–C bond breaking

mechanism. While other more complex mechanisms involving rearrangements may be possible, our proposed mechanism provides a simple and elegant explanation of VUV photodissociation of peptides leading to C–C bond breaking. UV photoionization may well be possible with Ala_Ala (calculated ionization energy of 8.1 eV comparable to the 157 nm UV laser). However, ionization energies that we calculated for the protonated peptides ($\text{Ala_Arg}(\text{H})^+ = 10.5$ eV, and $(\text{H})^+\text{Arg_Ala} = 10.9$ eV) are substantially larger, suggesting that direct electron detachment is not possible. However, even in the absence of direct photoionization, the behavior of the high-energy Rydberg excited states is expected to be similar to that of the ionized state and can play an important role in governing the fragmentation of peptides following VUV excitation. In the case of larger peptides with significant chain lengths, such a direct ionization process may be possible, though it is likely to occur away from the protonated residue, leading to C–C bond weakening.

UV excitation through a specific chromophore inducing a neighboring C–C bond dissociation has been investigated previously.^{21,22} For example, Lucas et al. carried out detailed investigations of photoinduced side-chain C–C bond breaking

(21) Cui, W.; Hu, Y.; Lifshitz, C. *Eur. Phys. J. D* **2002**, *20*, 565–571. Hu, Y. J.; Hadas, B.; Davidovitz, M.; Balta, B.; Lifshitz, C. *J. Phys. Chem. A* **2003**, *107*, 6507–6514.

in aromatic amino acids.²² Our primary focus in this investigation is to understand the general mechanism of photodissociation of peptides without requiring the presence of chromophores such as aromatic amino acids and independent of the charge location. In our general mechanism of photodissociation of peptides, in the absence of aromatic chromophores, the peptide bond absorbs the photon energy leading to excitation of a Rydberg state that has the characteristics of the corresponding cation. The resulting C–C bond elongation leads to electron delocalization and backbone C–C bond dissociation.

It is important to mention an additional surprising factor that emerges from our investigations. In Figure S3 of the Supporting Information, we show spin density distributions of the peptide ions in ionized and dissociative states. In particular, after breaking the C–C bond, it is interesting to observe the nature of the charged fragments and their subsequent behavior. In the case of the Ala_Ala peptide cation (Figure 1), analysis of fragment charges after the C–C bond dissociation shows that the C-terminal fragment gets the unpaired electron while the N-terminal fragment gains the positive charge, directly yielding an immonium ion ($\text{H}_2\text{N}^+=\text{CHR}$, Figure S4 of the Supporting Information). For the Ala_Arg(H)⁺ peptide ion (Figure S3a of the Supporting Information), the C-terminal arginine-containing part of the peptide will form the $x + 1$ radical ion after dissociation. Such a radical ion is a high-energy species that can undergo loss of hydrogen to form the x -ion seen experimentally. In larger peptides, loss of other small molecules can lead to rearranged species such as v - and w -type ions that are also frequently observed experimentally. More interestingly, when the N-terminus of this peptide becomes positively charged, it can form a stable immonium ion that may be detected experimentally. Unfortunately, in our experiments on Ala_Arg(H⁺), the low mass of the immonium ion ($m/e = 44$) precludes detection. Results obtained with the MP2/6-311++G(d,p) model are also consistent with this qualitative picture. More detailed analysis requires a careful study of the electron recapture process from the high-energy excited state during fragmentation.

Immonium ions that indicate the presence of individual amino acids are often detected when peptide ions are fragmented by high-energy processes.^{6,23} They offer important analytical information to confirm the presence of specific residues. In special cases, immonium ions have been observed via UV excitation of an aromatic chromophore leading to nearby side chain C–C fragmentation.^{21,22} b -Type ions commonly observed in low-energy peptide fragmentation can lose CO to yield a -ions, the smallest of which is an immonium ion.^{7,8,23,24} In our mechanism, a backbone C–C dissociation leads to the direct formation of an N-terminal immonium ion. It is consistent with the observation of immonium ions deriving from N-terminal residues that have been frequently observed in the electron ionization mass spectra of peptides.²⁵ In addition, immonium ions are often detected in the low-mass region of high-energy

MS spectra,²⁶ fully consistent with the electronic excitation/ionization occurring near the N-terminus if the charge is located at the C-terminus. High-energy collision-induced decomposition studies on small peptide ions showed the relative intensities of these immonium ions to be dependent on the positions of the amino acids in the peptide chain: C-terminal, N-terminal, or in-chain.²⁷ Thus, while there are many channels for the formation of immonium ions,^{7,8,21} the detection of N-terminal immonium ions is a natural consequence of our calculated mechanism.

Overall, many previous theoretical models, such as the “mobile proton model” for CID, charge and electron driven/remote models of ECD (electron capture dissociation), and so forth, can explain many unusual experimental observations of fragment ions including structural rearrangements.^{6–15,28} In this paper, we demonstrate a complementary mechanism for high-energy fragmentation in which electron excitation to nearly ionized states plays a central role and induces unusual backbone cleavage in protonated peptide ions. Observations of C–C backbone cleavage to yield a - and x -type product ions as well as immonium ions can now be relatively well understood. Studies on different combinations of dipeptides also suggest that similar electronic states are populated in all cases. We have also found that similar mechanisms for the backbone cleavages are valid in peptides of moderate length, and calculations are currently in progress in our laboratory on larger model systems.

Conclusions

Upon VUV excitation, peptide ions photodissociate at backbone C–C bonds resulting in a - or x -ion fragments. We suggest that laser induced fragmentation occurs via a Rydberg excitation (and/or electron detachment mechanism) and subsequent C–C bond cleavage. New experimental observations on protonated dipeptides provide a strong corroboration for our theoretical model. Our general results improve our understanding of the fundamental gas-phase chemistry of peptide ions and may help to evolve laser controlled chemistry of proteins and improve proteomics technology.

Acknowledgment. This work was supported by grants from the National Science Foundation (CHE-0616737 and CHE-0518234).

Supporting Information Available: Potential energy surfaces of bond dissociation in Ala_Arg and Arg_Ala peptide ions, spin density analysis and MP2 results on peptide ions, and complete ref 18. This material is available free of charge via the Internet at <http://pubs.acs.org>.

JA907975V

- (22) Lucas, B.; Barat, M.; Fayeton, J. A.; Perot, M.; Jouvet, C.; Gregoire, G.; Nielsen, S. B. *J. Chem. Phys.* **2008**, *128*, 164302.
(23) Ambihapathy, K.; Yalcin, T.; Leung, H. W.; Harrison, A. G. *J. Mass Spectrom.* **1997**, *32*, 209–215.
(24) Lam, A. K. Y.; Ramarathinam, S. H.; Purcell, A. W.; Ohair, R. A. J. *J. Am. Soc. Mass Spectrom.* **2008**, *19*, 1743–1754.

- (25) Speir, J. P.; Gorman, G. S.; Cornett, D. S.; Amster, I. J. *Anal. Chem.* **1991**, *63*, 65–69.
(26) Falick, A. M.; Hines, W. M.; Medzihradsky, K. F.; Baldwin, M. A.; Gibson, B. W. *J. Am. Soc. Mass Spectrom.* **1993**, *4*, 882–893.
(27) Madden, T.; Welham, K. J.; Baldwin, M. A. *Org. Mass Spectrom.* **1991**, *26*, 443–446.
(28) Antoine, R.; Broyer, M.; Chamot-Rooke, J.; Dedonder, C.; Desfrancois, C.; Dugourd, P.; Gregoire, G.; Jouvet, C.; Onidas, D.; Poulain, P.; Tabarin, T.; van der Rest, G. *Rapid Commun. Mass Spectrom.* **2006**, *20*, 1648–1652.